Analytical Investigation of Thermal Contact Resistance (TCR) Behavior under Time-Dependent Thermal Load

Mehran Ahmadi[†], Mohammad Fakoor Pakdaman[‡]. Majid Bahrami[†1]
[†] *Laboratory for Alternative Energy Conversion* (LAEC)
School of Mechatronic Systems Engineering, Simon Fraser University (SFU)
Surrey, BC, Canada
[‡] Department of Mechanical Engineering, British Columbia Institute of Technology (BCIT)
Burnaby, BC, Canada
mahmadi@sfu.ca, mfakoorpakdaman1@sfu.ca, mbahrami@sfu.ca

Abstract

Thermal contact resistance under general time-dependent thermal load is investigated in this study. Assuming known number of contacts points, and the average surface area of each contact, the focus of this study is on the thermal aspect of contact resistance, i.e. spreading/constriction resistance at the contact point. A general analytical solution for thermal spreading/constriction resistances of a time-dependent circular source on a finite circular cylinder with uniform side and end cooling is presented. The solution is applicable to a general axisymmetric heat flux distribution, including both isoflux and isothermal distributions. The time response of the flux tube under different geometrical and boundary conditions is investigated and the result are shown. The results are also compared to, and successfully verified by an independent numerical simulation.

Keywords

Thermal contact resistance, Spreading resistance, Dynamic thermal load, Analytical solution, Numerical simulation

1. Introduction

Thermal management of electronics and power electronics has vast applications in several industries such as; telecom industry (datacenters and outdoor enclosures), automotive industry (conventional vehicles, hybrid vehicles, electric vehicles, and fuel cell vehicles), renewable energy systems (solar panels and wind turbine power electronics), aerospace industry, and light-emitting diode (LED) industry. Efficient thermal management of electronics is essential for optimum performance and durability. About 55% of failures in electronics during operation have a thermal root [1]. The rate of failures due to overheating nearly doubles with every 10°C increase above the operating temperature [2]. Considering the increasing functionality and performance of electronic devices and the ever increasing desire for miniaturization in the industry, thermal management has become the limiting factor in the development of such devices, [3–5], and reliable low-cost cooling methods are more and more required. The main goal of electronics cooling is the effective transfer of heat from source, e.g. IGBTs or MOSFETs to the ambient heatsinks or other cooling systems. The effectiveness of this procedure highly depends on the system's total thermal resistance, which is composed of discrete thermal resistances on the path of heat from source to ambient. One of the major resistances is thermal contact resistance (TCR). Heat transfer across an interface formed by two contacting solid bodies is usually accompanied by a measurable temperature difference because there exists a thermal resistance to heat flow in the region of the interface. It is a well-known fact that all engineering surfaces exhibit waviness and roughness, as the result of the inherent action of production processes and warping strains. As a result of these surface asperities, when two solid bodies are brought together under a load, there will be intimate contact at many small discrete spots, and a gap will exist in the regions of no real contact (see **Figure 1**). The gap region will normally be occupied by a fluid, such as air.

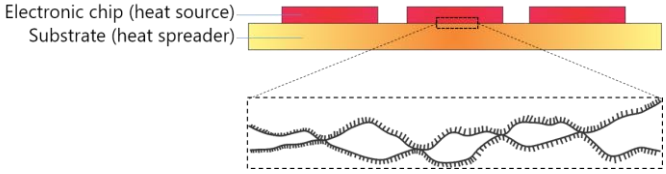

Figure 1: Schematic of contact geometry when two solid bodies are brought together.

The brief review of **Figure 1**, clearly shows that the contact phenomenon is quite complex, since there are many parameters such as: apparent contact pressure, thermal conductivity of the solid bodies, surface roughness and waviness, material elasticity and plasticity, number and geometry of the contact spots, etc., that affect the transport of heat across the interface. As such, it is necessary to separate this phenomenon into three principal problems: i) mechanical problem, ii) thermal problem, and iii) metrology: surface description and measurement. It would be wrong to believe that only one theory could predict the thermal resistance over all possible ranges, as each area requires special expertise and considerations in order to evaluate the relative importance of one parameter over another. For more introductory information on mechanical and metrology aspects of the problems, the reader is invited to see Yvanovich *et al*. work [6] on calculating the interface resistance. The focus of this study is the thermal problem, in which the major part is the heat spreading/constriction resistance at the contact spots (see **Figure 2**). In this study we assume that the surface characteristics are measured and the mechanical problem is

[1] Corresponding author
Email:mbahrami@sfu.ca

solved through Hertzian contact theory or any other mechanical model [7], meaning that the number and the average surface area of contact points are known. This study focuses on solving the thermal aspect of the problem, i.e. spreading/constriction resistance in one contact point. As shown in **Figure 2**, due to less resistance through the contact points in an solid-solid interface, the heat transfer mainly occurs through these area, which causes spreading/constriction of constant heat flux lines. This geometry-imposed bottleneck causes the heat not to distribute uniformly in the system and introduces an extra resistance to the system. There are other mechanisms for the interfacial heat transfer such as: radiation between the gap surfaces and conduction through the fluid inside the gaps, which are not considered in this study to simplify the problem. The role of radiation and conduction through the gaps become more important at considerably high temperatures and high fluid pressures, respectively, which is not the case for many engineering applications, specifically electronics cooling. So the focus of this paper is spreading/constriction resistance as the major thermal contributor to the thermal contact resistance (TCR). In this study, the geometry of the contact spots is assumed to be circular (**Figure 2**); however, other geometries such as ellipse, rectangle and line are also possible to be formed in the contact area.

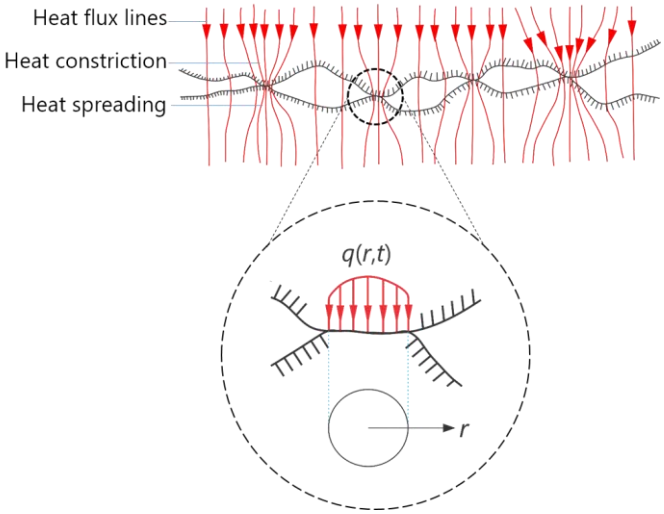

Figure 2: constriction and spreading of at the contact areas of the surface interface. Magnified region is a representative unit cell of a contact point with circular contact area.

Many researchers studied different aspects of contact resistance via. spreading/constriction resistances of a circular area subjected to different boundary conditions [8,9]. The solutions have mainly been reported for steady-state heat conduction into the four regions, defined as: i) isotropic half-space, ii) semi-infinite circular flux tube, iii) thin disk of infinite extent, and iv) finite length circular cylinder with different film coefficients imposed on the side and end surfaces. Mikic and Rohsenow [10] obtained analytical relations for spreading resistances for a circular heat source on one end of a semi-infinite flux tube and a finite length finite flux tube. They reported solutions for the isoflux source and the quasi-isothermal source based on the equivalent isothermal flux distribution for the insulated boundary condition on the side. Yovanovich [11] developed a general analytical solution for the dimensionless steady-state spreading resistances for a general, axisymmetric heat flux distribution, $q(r)$, over a circular source on a semi-infinite flux tube. In another study, Yovanovich [12] presented an integral method for finding the spreading resistances of single planar isoflux sources of arbitrary shape placed on isotropic half-space. Yovanovich and Burde [13] used an integral method [12] to find the dimensionless spreading resistances of several non-symmetric, isoflux sources based on the centroid and average temperature basis. They used the square root of the source area as the characteristics length scale for nondimensionalization, and reported that heat sources with the same area and aspect ratio, e.g. a circle and a square, had spreading resistances that differed by less than 1–2%. Martin *et al.* [14] used the method of moments to find spreading resistances for several source geometries such as circle, square and equilateral triangle. They obtained numerical results for isothermal and isoflux boundary conditions. Yovanovich [15] presented a general solution for thermal spreading resistances of a circular source on a finite circular cylinder with uniform side and end cooling. He showed that several special cases presented by many researchers arise directly from his general solution. More extensive literature review on steady state spreading/constriction resistances can be found on [15].

A number of studies have also focused on transient spreading/constriction resistance within isotropic materials. Turyk and Yovanovich [16] reported the analytical solutions for transient spreading resistances within semi-infinite circular flux tubes and two-dimensional channels. Yovanovich [17] used surface element method to report approximate solution to transient temperature rise of arbitrary contacts with uniform flux. Kadambi and Abuaf [18] used the method of separation of variables (SOV) to report the transient temperature distribution in a finite circular cylinder with insulated side and uniform end cooling, and a circular constant heat source on top.

This brief review of the pertinent literature shows that in spite of over six decades of research on systems consisting of a single heat source on substrates, time dependent contact resistance, thus spreading/constriction, has not been investigated to date. Considering the recent turn of industry towards sustainable energy resources, time-dependent thermal studies of energy systems seem to become an inevitable topic in engineering [2]. Resources such as wind and solar energy have a very time-dependent behavior in term of availability. Electric vehicles as another example, due to the highly time-varying power demand of driving cycles, go through time-dependent energy cycles [19]. This change of available/demanded energy with time, imposes a time-varying load cycle on all components including the electronics and consequently electronics cooling systems [20,21]. Therefore, the thermal contact resistance which in this study gets narrowed to spreading/constriction resistances, as one of the major barriers in heat transfer path inside the cooling systems, is required to be studies under time-varying thermal loads. To address this shortcoming, this study aims to present a new general analytical solution for time-dependent

spreading/constriction resistance. This study is the extension of Yovanovich's work [15] by assuming the boundary source, as a function of both time and space. This makes the presented solution a more general case, being applicable to calculation of spreading/constriction resistance under time-varying thermal load. The general solution will give the time-dependent temperature response of the system to the boundary condition at different locations. It is worth mentioning that due to the analogy between the heat transfer and charge transfer in the solids, the same solutions can be used for the concept of electrical contact resistance (ECR). In fact, the solution to this problem can be applied to any diffusion problem, including the interface resistance against the mass transfer. To define the problem geometry and the boundary conditions, the magnified section in the **Figure 2**, can be shown in more mathematical-friendly form, as shown in **Figure 3**. This geometry is also known as "flux tube". More details on the solution domain, boundary conditions, and problem definition are brought in section 2.

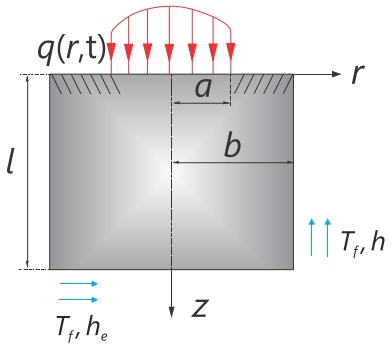

Figure 3: Schematic of the problem; finite flux tube with side and end cooling.

2. Problem definition

The geometry shown in **Figure 3**, represents one contact spot at the interface between two mating surfaces. It consists of a circular source of radius a on one end of a finite cylinder of radius b, with thickness l, and thermal conductivity k. The sides, $r=b$, and the end $z=l$ are cooled by a fluid at fixed temperature T_f through uniform, but different heat transfer coefficients h and h_e, respectively. It should be noted that in a contact resistance problem, there is no side cooling. However, to make the solution more general, we considered the side and end cooling. The side or end boundary conditions can be changed to insulated at the limiting case of h approaching zero. The axisymmetric time-depending heat flux over the source area has the following general form

$$q(r,t)=\frac{Q(1+\mu)}{\pi a^2}\left[1-\left(\frac{r}{a}\right)^2\right]^{\mu}\left[1+\cos(\omega t)\right] \quad for \quad 0<r<a/b \qquad (1)$$

where Q is the total heat transfer rate from the source into the system, and μ is the heat flux distribution parameter. Three interesting distributions are obtained when μ = -1/2, 0, 1/2. The flux distribution corresponding to μ = -1/2 has a minimum at the center (r=0) and is unbounded at the edge of the heat source (r=a). This flux distribution is frequently used to approximate an isothermal source area [22]. The distribution corresponding to μ = 0 represent an isoflux distribution at steady-state. The third flux distribution corresponding to μ = 1/2 is parabolic; it has a maximum at the center and goes to zero at the edge of the source area. In this study, cosine function is chosen to represent time-dependency of the boundary condition. It should be noted that using cosine Fourier transform any kind of time-dependent function can be re-written in the form of a cosine function. All the boundary conditions of this problem are tried to be selected as general as possible to cover a whole range of possible scenarios. For example, by setting the heat transfer coefficient, h, at the side to zero, the insulated boundary condition can be achieved; at the other limit where coefficient, h_e, at the bottom approaches infinity, the constant temperature boundary condition at $z = L$ can be achieved.

3. Governing equation, initial and boundary conditions

The governing differential equation for the axisymmetric temperature rise $\theta(r,z,t) = T(r,z,t) - T_f$ is

$$\frac{1}{r}\frac{\partial}{\partial r}\left(r\frac{\partial\theta}{\partial r}\right)+\frac{\partial^2\theta}{\partial z^2}=\frac{1}{\alpha}\frac{\partial\theta}{\partial t}, \quad 0\le r\le b, \quad 0\le z\le l \qquad (2)$$

The initial and boundary conditions are

$$\begin{aligned}
&t=0, \quad \theta=0\\
&r=0, \quad \frac{\partial\theta}{\partial r}=0\\
&r=b, \quad \frac{\partial\theta}{\partial r}=-Bi\,\theta\\
&z=0, \quad \frac{\partial\theta}{\partial z}=\begin{cases}-\dfrac{q(r,t)}{k}, & 0\le r\le a\\ 0, & a\le r\le b\end{cases}\\
&z=l, \quad \frac{\partial\theta}{\partial z}=-Bi_e\theta
\end{aligned} \qquad (3)$$

where Bi=hb/k and Bi_e=h_eb/k are the Biot numbers on the side and the end of the cylinder, respectively.

3.1. Steady-state solution

Using method of separation of variable (SOV) and Fourier-Bessel expansion, Yovanovich [15] reported the steady state solution with boundary condition on the circular source of,

$$q(r)=\frac{Q(1+\mu)}{\pi a^2}\left[1-\left(\frac{br}{a}\right)^2\right]^{\mu} \qquad (4)$$

and presented the temperature distribution inside the cylinder in the following form:

$$\theta(r,z)=\sum_{n=1}^{\infty}A_nJ_0(\lambda_n r)\left[\cosh(\lambda_n z)-\varphi_n\sinh(\lambda_n z)\right] \qquad (5)$$

$$\varphi_n=\frac{Bi_e+\delta_n\tanh(\delta_n\tau)}{\delta_n+Bi_e\tanh(\delta_n\tau)} \qquad (6)$$

where $\tau = l/b$, and eigenvalues, λ_n, are the positive roots of the characteristic equation:

$$\delta_nJ_1(\delta_n)=Bi\,J_0(\delta_n) \qquad (7)$$

with $\delta_n = b\,\lambda_n$ and J_0 and J_1 are Bessel function of first kind of order zero and one respectively. A_n is defined as:

$$A_n=\frac{2Q}{a\pi k}\left(\frac{2}{\delta_n\varepsilon}\right)^{\mu}\frac{\Gamma(2+\mu)J_{1+\mu}(\delta_n\varepsilon)}{\varphi_n\delta_n^2\left(J_0^2(\delta_n)+J_1^2(\delta_n)\right)} \qquad (8)$$

with $\varepsilon = a/b$ and Γ being the Gamma function.

3.2. Transient solution

Before solving the problem with periodic flux at the boundary, we need to solve the transient problem with the following boundary condition at $z = 0$:

$$q(r) = \frac{Q(1+\mu)}{\pi a^2}\left[1-\left(\frac{br}{a}\right)^2\right]^{\mu} \tag{9}$$

The transient solution related to the system start up, where the response of the system to the applied boundary condition is a matter of interest, from the beginning of the process until the steady-state condition is reached. The rest of boundary conditions and the governing equation will remain unchanged as appeared in Eq. 3. We start solving the problem by assuming that the final solution $\theta(r,z,t)$ is separable into a steady-state and a transient part.

$$\theta(r,z,t) = \theta_t(r,\mathrm{z},\mathrm{t}) + \theta_s(r,z) \tag{10}$$

The steady-state temperature, θ_s, is reported in section 3.1, Eq. 5. By substituting Eq. 10 into Eq. 2, the governing equation can be re-written as

$$\frac{1}{r}\frac{\partial}{\partial r}\left(r\frac{\partial \theta_t}{\partial r}\right)+\frac{\partial^2 \theta_t}{\partial z^2} = \frac{1}{\alpha}\frac{\partial \theta_t}{\partial t} \tag{11}$$

Boundary conditions for the transient solution, θ_t, can be rearranged as:

$$\begin{aligned}
&t=0, \quad \theta = 0 \quad so \quad \theta_t = -\theta_s \\
&r=0, \quad \frac{\partial \theta}{\partial \bar{r}} = 0 \quad so \quad \frac{\partial \theta_t}{\partial r} = -\underbrace{\frac{\partial \theta_s}{\partial r}}_{=0} \quad so \quad \frac{\partial \theta_t}{\partial r} = 0 \\
&r=b, \quad \frac{\partial \theta}{\partial r} = -Bi\,\theta \quad so \quad \frac{\partial \theta_t}{\partial r} = -Bi\,\theta_t \\
&z=0, \quad \frac{\partial \theta}{\partial z} = \begin{cases} -\dfrac{q(r,t)}{k}, & 0 \le r \le a \\ 0, & a \le r \le b \end{cases}, \quad so \quad \frac{\partial \theta_t}{\partial z} = 0 \\
&z=l, \quad \frac{\partial \theta}{\partial z} = -Bi_e\,\theta \quad so \quad \frac{\partial \theta_t}{\partial z} = -Bi_e\,\theta_t
\end{aligned} \tag{12}$$

The method of separation of variables can be employed to solve Eq. 11 subjected to boundary conditions, Eq. 12.

$$\theta_t(r,z,\mathrm{t}) = \Upsilon(r)Z(z)\Lambda(t) \tag{13}$$

To solve for $\Upsilon(r)$ and $Z(z)$ we use an Eigenfuction expansion method [23]. Auxiliary equations can be written in both r-direction and z-direction:

r-direction $$\frac{1}{r}\frac{d}{dr}\left(r\frac{d\Upsilon}{dr}\right) = -\lambda^2\Upsilon \tag{14}$$

z-direction $$\frac{d^2 Z}{dz^2} = -\gamma^2 Z \tag{15}$$

After applying the boundary conditions to the auxiliary Eqs. 14 and 15, and using the governing Eq. 11, functions $R(r)$ and $Z(z)$ can be found as:

r-direction $$\Upsilon(r) = J_0(\lambda_n r) \tag{16}$$

z-direction $$Z(z) = \cos(\gamma_m z) \tag{17}$$

where the eigenvalues λ_n and γ_m are the positive roots of Eqs. 18 and 19, respectively:

r-direction $$\delta_n J_1(\delta_n) = Bi J_0(\delta_n) \tag{18}$$

z-direction $$\eta_m \tan(\eta_m \tau) = Bi_e \tag{19}$$

with $\eta_m = b\,\gamma_m$. Substituting Eqs. 16 and 17 into Eq. 11, $\Lambda(t)$ can be found as

$$\Lambda(t) = B_{mn}\exp\left[-\alpha\left(\lambda_n^{\,2}+\gamma_m^{\,2}\right)t\right] \tag{20}$$

and consequently $\theta_t(r,z,t)$ will be

$$\theta_t(r,z,t) = \sum_{n=1}^{\infty}\sum_{m=1}^{\infty} B_{mn}J_0(\lambda_n r)\cos(\gamma_m z)\exp\left[-\alpha\left(\lambda_n^{\,2}+\gamma_m^{\,2}\right)t\right] \tag{21}$$

Substituting the initial condition, B_{mn}:

$$B_{mn} = \frac{\int_0^l A_n\left\{\cosh(\lambda_n z) - \dfrac{Bi_e + \delta_n \times \tanh(\delta_n \tau)}{\delta_n + Bi_e \times \tanh(\delta_n \tau)}\sin(\lambda_k z)\right\}\cos(\gamma_m z)\,dz}{\int_0^l \cos^2(\gamma_m z)\,dz} \tag{22}$$

3.3. General time-dependent solution

After finding the transient solution, Duhamel's theorem [23] can be used to find the general solution for the cosine form of the boundary condition:

$$q(r) = \frac{Q(1+\mu)}{\pi a^2}\left[1-\left(\frac{br}{a}\right)^2\right]^{\mu}\left[1+\cos(\omega \mathrm{t})\right] \tag{23}$$

After applying Duhamel's theorem and integrating over time, the final form of the solution will be

$$\theta(r,z,t) = -\sum_{n=1}^{\infty}\sum_{m=1}^{\infty}\alpha B_{mn}\left(\lambda_n^{\,2}+\gamma_m^{\,2}\right)J_0(\lambda_n \mathrm{r})\cos(\gamma_m \mathrm{z})\left\{\begin{array}{l} \dfrac{\alpha\omega\left(\lambda_n^{\,2}+\gamma_m^{\,2}\right)\sin(\omega t)+\alpha^2\left(\lambda_n^{\,2}+\gamma_m^{\,2}\right)^2\cos(\omega t)+\left(\lambda_n^{\,2}+\gamma_m^{\,2}\right)+\omega^2}{\left[\alpha^2\left(\delta^2+\gamma^2\right)^2+\omega^2\right]\alpha\left(\lambda_n^{\,2}+\gamma_m^{\,2}\right)} \\ -\dfrac{\left[\alpha^2\left(\delta^2+\gamma^2\right)^2+\omega^2\right]\exp\left[-\alpha\left(\lambda_n^{\,2}+\gamma_m^{\,2}\right)t\right]}{\left[\alpha^2\left(\delta^2+\gamma^2\right)^2+\omega^2\right]\alpha\left(\lambda_n^{\,2}+\gamma_m^{\,2}\right)} \end{array}\right\} \tag{24}$$

3.4. System thermal contact resistance

The total resistance of the system is defined with respect to the mean temperature rise of the source area

and

$$R_{sys} = \frac{\theta_{avg}}{Q} \tag{25}$$

where R_{sys} is the flux tube total resistance. The total resistance is equal to the spreading resistance plus the one-dimensional conduction resistance along the tube:

$$R_{sys} = R_s + \frac{l}{k\pi b^2} \tag{26}$$

with R_s being spreading resistance.

4. Numerical simulation

An independent finite element numerical simulation was prepared in COMSOL Multiphysics to validate the results of the present analytical solution. Different number of mesh elements was tested and the results were compared for the maximum local temperature (at $r = 0$ and $z = 0$) to ensure mesh independency. Accordingly, choosing a mesh size of 2×10^4, we found a maximum 2% deviation in the temperature values compared to the simulation of cylinder with a mesh

number of 3×10^4. Similarly, the maximum temperature for the simulation with 1×10^4 mesh elements deviated up to 1.5% as compared to those from the finest mesh size. Therefore, we chose a mesh size of 2×10^4 elements considering that it was sufficient for the numerical investigation purposes.

The comparison between the analytical solution, Eq. 24, and numerical results is shown in **Figure 4**. The values shown in **Figure 4** are for a case with Bi = 0.0001that is associated with insulated boundary condition on the side of cylinder. Several other simulations under different boundary conditions are also performed and compared them the analytical solutions for further validation. The boundary conditions and thermophysical properties are shown in **Figure 4**. The maximum relative difference between the numerical and analytical results is less than 5%.

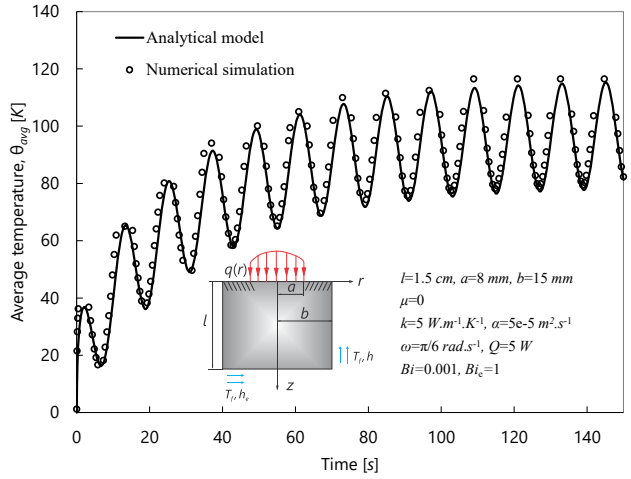

Figure 4: A comparison between the analytical solution and numerical data, with maximum, minimum, and average relative differences of 4.9%, 0.8%, and 2.1% respectively.

5. Results and discussion

Thermal lag; **Figure 5** shows the imposed source heat flux and the temperature response on the axis at the bottom of the cylinder. As shown in **Figure 5**, there is a phase shift between the imposed boundary condition and the thermal response of the flux tube. This lag can be interpreted as the thermal inertia effect, i.e., density times specific heat capacity ($\rho.c_p$).

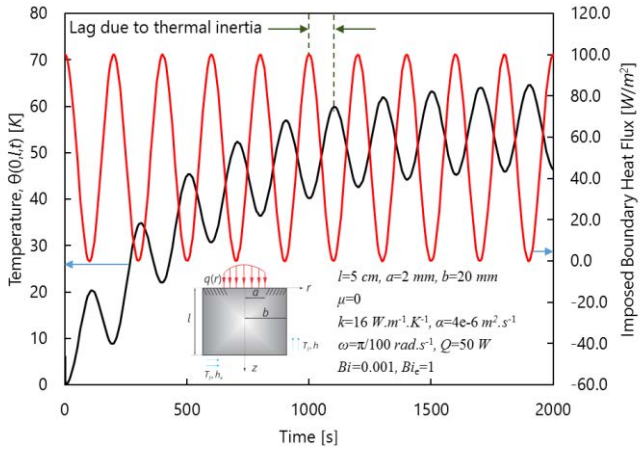

Figure 5: Effect of thermal inertia on tube flux response,; the temperature at $r = 0$, $z = l$, and the source heat flux imposed.

Effect off aspect ratio ε: Figure 4 shows the effect of aspect ratio, ε = a/b. This can also be viewed as the ratio of real to nominal contact area at the contacting surfaces. As per Bahrami *et al.* [7], in most engineering applications, the real contact area is less than 2% of the nominal contact area. As it is expected, smaller aspect ratios cause more resistance for heat transfer which leads to an increase in spreading resistance and consequently the total resistance.

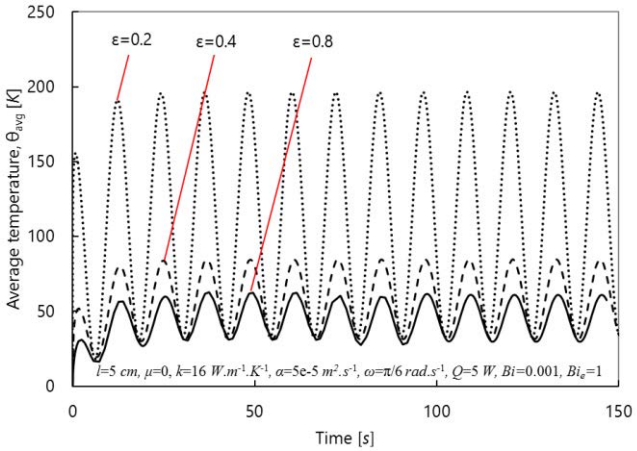

Figure 6: The effect of ε = a/b on spreading resistance of the system.

Effect of Bi_e: Average temperature at the bottom of the flux tube, z=l as a function of time is shown in **Figure 7**. As expected, higher values of Biot number cause less temperature difference between the bottom of cylinder and the ambient. Using a convective cooling boundary condition at the side and the end of cylinder makes the solution more general, since very low values of Biot number can resemble the adiabatic boundary condition, q=0, and very high values of Biot can simulate the constant temperature boundary condition, T=T_f.

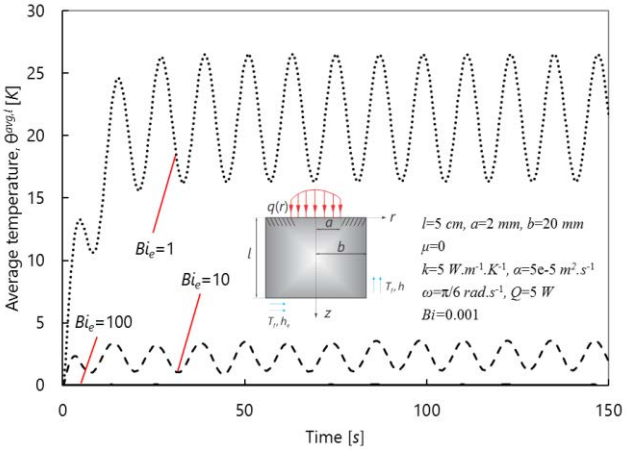

Figure 7: Average temperature at $z = l$ versus time, the effect of Bi_e on average end temperature.

Effect of frequency: The effect of frequency of the source heat flux is studied at Figure 8. Two asymptotes can be identified, when the angular frequency approaches to its limiting cases. Both asymptotes resemble the solution to the step function boundary condition, but with different

amplitudes. At very small frequencies when ω approaches zero, the source heat flux becomes: $q(r)=[1+\cos(\omega t)]$, the temperature response would be in the form of the response to a step function but with amplitude twice as large as the amplitude of the original source boundary condition. At the other limit, at very large frequencies due to thermal inertia, the temperature response cannot follow the fluctuations at the source, thus its behaviour resembles the response to a step function with amplitude identical to the original boundary condition.

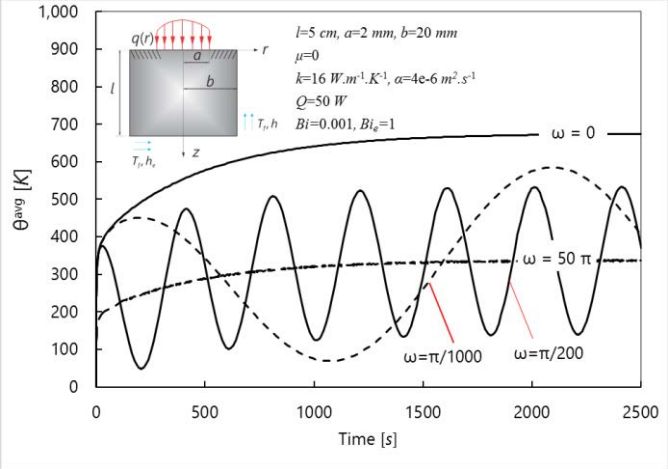

6. Figure 8: The effect of angular frequency on the time response of system.

7. Conclusion

For the first time in the literature the time-dependent spreading/constriction resistances is studied for circular source on a finite circular cylinder with uniform side and end cooling. A general boundary condition was used for the circular source, to be able to resemble both heat flux and temperature boundary condition. The problem is solved for the general convective cooling conditions, which allows the modification of the solution for insulated and constant temperature of side and end, by letting the heat transfer coefficient go to zero (very small values) and infinity (very large values) respectively. Combined with a mechanical model to account for the number and the actual surface area of contact points at the interface, the presented thermal solution can provide a general analytical solution for calculation of thermal contact resistance under arbitrarily time-varying thermal load and various boundary conditions. Our study shows that the first sixty term of the series are enough for accurate results up to 4 decimal digits. An independent numerical simulation is also prepared, and the results from analytical solution are successfully verified against numerical data. Parametric study was performed on the important parameters and the following highlights were observed;

- There is a time lag between the fluctuations at boundary and the temperature response of the system. The higher the thermal inertia, $\rho.c_p$, the bigger the thermal lag.
- The ratio between the source area and the cylinder cross section area affects the spreading resistance significantly. The higher the value of $\varepsilon = a/b$, the higher the value of spreading resistance.
- At very low frequencies the system response would change to the temperature response to a step function boundary condition, since the effect of fluctuations are negligible.
- At very high frequencies the thermal inertia prevents the system from following the fluctuations at the boundary and the system response would get closer to response to a step function.

8. References

[1] Anandan, S., and Ramalingam, V., 2008, "Thermal management of electronics: A review of literature," Int. J. Therm. Sci., **12**(2), pp. 5–26.

[2] Gurrum, S. P. S., Suman, S., Shivesh, K., Joshi, Y. K., and Fedorov, A. G., 2004, "Thermal Issues in Next-Generation Integrated Circuits," IEEE Trans. DEVICE Mater. Reliab., **4**(4), pp. 709–714.

[3] Wankhede, M., Khaire, V., and Goswami, A., 2007, "evaluation of cooling solutions for outdoor electronics," 13th International Conference on Thermal Investigation of ICs and Systems, ©EDA Publishing, Budapest, Hungary, pp. 1–6.

[4] Jahkonen, J., Puolakka, M., and Halonen, L., 2013, "Thermal Management of Outdoor LED Lighting Systems and Streetlights Variation of Ambient Cooling Conditions," LEUKOS, **9**(3), pp. 155–176.

[5] Christensen, A., Ha, M., and Graham, S., 2007, "Thermal Management Methods for Compact High Power LED Arrays," 7th International Conference on Solid State Lighting, I.T. Ferguson, N. Narendran, T. Taguchi, and I.E. Ashdown, eds., SPIE UK, San Diego, California, USA, p. 66690Z–66690Z–19.

[6] Yovanovich, M. M., Culham, J. R., and Teertstra, P., 1997, "Calculating interface resistance," Electron. Cool., **54**(1), pp. 1–9.

[7] Bahrami, M., Yovanovich, M., and Culham, J., 2005, "Thermal contact resistance at low contact pressure: Effect of elastic deformation," … J. heat mass Transf., **48**(16), pp. 3284–3293.

[8] Bejan, A., and Kraus, A., 2003, Heat transfer handbook, JOHN WILEY & SONS, INC.

[9] Rohsenow, W. M., Hartnett, J. P., and Cho, Y. I., 1998, Handbook of heat transfer, McGraw-Hill.

[10] Mikic, B. B., and Rohsenow, W. M., 1966, Thermal Contact Resistance, Cambridge MA.

[11] Yovanovich, M. M., 1967, "General Expressions for Constriction Resistances of Arbitrary Flux Distributions," Radiat. Transf. Therm. Control, **49**, pp. 381–396.

[12] Yovanovich, M. M., 1976, "Thermal Constriction of Contacts on a Half- Space: Integral Formulation," Radiat. Transf. Therm. Control, **49**, pp. 397–418.

[13] Yovanovich, M. M., and Brude, S. S., 1977, "Centroidal and Area Average Resistances of Nonsymmetric, Singly Connected Contacts," AIAA J., **15**(10), pp. 1523–1525.

[14] Martin, K. A., Yovanovich, M. M., and Chow, Y. L., 1984, "Method of Moments Formulation of Thermal

Constriction Resistance of Arbitrary Contacts," AIAA Pap., **84**(5), pp. 25–28.
[15] Yovanovich, M. M., 2003, "Thermal Resistances of Circular Source on Finite Circular Cylinder With Side and End Cooling," J. Electron. Packag., **125**(2), p. 169.
[16] Turyk, P. J., and Yovanovich, M. M., 1984, "Transient Constriction Resistance for Elemental Flux Channels Heated by Uniform Heat Sources," 52nd ASME Heat Transfer Conference, ASME, New York.
[17] Yovanovich, M. M., and Negus, K., 1984, "Transient Temperature Rise of Arbitrary Contacts with Uniform Flux by Surface Element Methods," AIAA 22nd Aerospace Sciences Meeting, Reno, NV, pp. 1–7.
[18] Kadambi, V., and Abuaf, N., 1985, "An Analysis of the Thermal Response of Power Chip Packages," IEEE Trans. Electron. Devices, **32**(6), pp. 1024–1033.
[19] Kelly, K. J., Abraham, T., Bennion, K., Bharathan, D., Narumanchi, S., and O'Keefe, M., 2007, "Assessment of thermal control technologies for cooling electric vehicle power electronics," Twenty third International Electric Vehicle Symposium (EVS-23), Anaheim, CA.
[20] McGlen, R. J., Jachuck, R., and Lin, S., 2004, "Integrated thermal management techniques for high power electronic devices," Appl. Therm. Eng., **24**(8-9), pp. 1143–1156.
[21] Brooks, D., and Martonosi, M., 2001, "Dynamic thermal management for high-performance microprocessors," Proceedings HPCA Seventh International Symposium on High-Performance Computer Architecture, pp. 171–182.
[22] Yovanovich, M. M., Culham, J. R., and Teertstra, P., 1998, "Analytical modeling of spreading resistance in flux tubes, half spaces, and compound disks," IEEE Trans. Components, Packag. Manuf. Technol. Part A, **21**(1), pp. 168–176.
[23] Carslaw, S. H., and Jagear, J. C., 1959, Conduction of Heat in Solids, Oxford Press, London, UK.